

Reactivity in the Solid State Between Cobalt and Aluminum Molybdate

M. Kassem

(Submitted February 18, 2010; in revised form June 29, 2010)

The reactivity of aluminum molybdate with cobalt was studied. Pure materials have been synthesized by the solid state method using Al_2O_3 and MoO_3 in proportional quantities. The product then mixed with different quantities of Cobalt in molar ratio ($\text{Co}/\text{Al}_2(\text{MoO}_4)_3 = 0, 0.1, 0.2, 0.3, 0.4, 0.5, 0.6, 0.8$ and 1). The pure initial and resultant materials were characterized using powder x-ray diffraction, Fourier transform IR (FTIR), differential thermal analysis (DTA) and nitrogen adsorption. The results suggest that Co, when mixed at fixed temperature with $\text{Al}_2(\text{MoO}_4)_3$ in the solid state, does not remain inert. This statement is based on the absence of any detectable free cobalt in any sample by the techniques which were employed. Two other phases CoMoO_4 and MoO_2 appear gradually besides the original phase, with increasing the molar ratio. The CoMoO_4 starts to appear overall the used molar ratio range while MoO_2 shows up only for molar ratio higher than 0.6 . The appearance of these two phases, detected by x-ray diffraction, has also been confirmed by FTIR and DTA measurements. The reactivity of cobalt towards aluminum molybdate is manifested also by the modification of the adsorption isotherm and pore size distribution where a mesoporosity has been clearly shown for samples containing molar ratio higher than 0.6 .

Keywords aluminum molybdate, cobalt, phase equilibrium

1. Introduction

There is a continuing need to find new ion exchangers which are capable of treating radioactive nuclear waste and to remove toxic substances from aqueous effluents. In particular, there is a requirement to remove certain transition metal ions such as cobalt and nickel from the cooling water of nuclear power stations.

Inorganic adsorbents, having pores or channels in their structures, such as TiO_2 , Al_2O_3 and ZrO_2 have been investigated for use in this purpose.^[1-7] The cobalt ions were chemisorbed on these materials as cobalt meta zirconate CoZrO_3 and meta titanate CoTiO_3 or spinel-type compounds such as CoAl_2O_4 .

Significant importance results from the valuable qualities of new inorganic adsorbents, the investigation of materials containing molybdate of trivalent metals such as $\text{Al}_2(\text{MoO}_4)_3$ is of interest in relation to the sorption of cobalt. This is due to its low solubility in water or low acidic solution and due to its particular crystal structure. The crystal structure of this compound, as described by William T.A.Harrison and his co-workers,^[8] is monoclinic, space group $P121/A1$ (No. 14), $a = 1.53803(9)$ nm, $b = 0.90443(1)$ nm, $c = 1.7888(1)$ nm, $\beta = 125.382(2)^\circ$, $V = 1.03108(9)$. It is an open framework of

octahedral AlO_6 and tetrahedral MoO_4 building blocks which are fused together by Al-O-MO bonds. The $\text{Al}_2(\text{MoO}_4)_3$ open framework favors accommodation of mobile cation such as Co^{2+} .

Thus it seemed advisable to find, as an objective of this work, how $\text{Al}_2(\text{MoO}_4)_3$ would behave towards different quantities of cobalt when it accommodates them in its framework.

2. Experimental

Powder samples of $\text{Al}_2(\text{MoO}_4)_3$ were prepared by solid-state methods. Stoichiometric molar ratio of the precursor oxides (analytical grade) were mixed and thoroughly ground, prior to firing for 2 days at 750°C .^[9] The reaction of $\text{Al}_2(\text{MoO}_4)_3$ with cobalt was performed by mixing, in solid state, a fixed quantity of the prepared $\text{Al}_2(\text{MoO}_4)_3$ with different quantities of cobalt in molar ratio $\text{Co}/\text{Al}_2(\text{MoO}_4)_3 = 0, 0.1, 0.2, 0.3, 0.4, 0.5, 0.6, 0.8$ and 1 . Each mixture was afterwards heated at temperature of 750°C in a sealed tube for 3 days.

Powder x-ray diffraction (XRD) patterns were recorded on a STADI-P STOE Transmission diffractometer, using Cu K α radiation ($\lambda = 0.154059$ nm), and a germanium monochromator operated at 50 kV and 30 mA. XRD patterns were measured between 5° and $90^\circ 2\theta$, with a step size of 0.01 and a scanning speed of $0.5^\circ/\text{min}$. The quantitative phase analysis was performed using Stoe-winXpow 32 Software which uses the reference intensity ratio method and stored I/I_{cor} values of identified phase.^[10]

Absorption bands were also recorded between 400 and 4000 cm^{-1} by a Fourier transform IR (FTIR) spectrometer

M. Kassem, Chemistry Department, Atomic Energy Commission of Syria, P.O. Box 6091 Damascus, Syria. Contact e-mail: cscientific@aec.org.sy.

Section I: Basic and Applied Research

in the transmittance mode (Bruker IFS66). The samples were prepared as KBr discs containing 0.001 g of the samples. All spectra have been obtained at room temperature with a resolution of 2 cm^{-1} .

Nitrogen adsorption and desorption measurements were made using an automated surface area and pore structure analyzer (Quantachrome NOVA 2200) at 77 K, the instrument has been calibrated with standard reference material of Al_2O_3 .

Prior to analysis 0.15-0.18 g of samples was degassed at 100 °C for at least 4 h under vacuum (10^{-3} Torr).

An adsorption-desorption isotherm was also determined for each of the samples using 20-points within the range $P/P_0 = 0.02-0.50$ and the BET method.^[11] The pore diameter distribution was determined using the BJH method.^[12]

Differential thermal analyses curves of the prepared samples were performed using a Shimadzu DT 40 thermal analyzer under air with heating rate of 10 °C/min in the 20-900 °C temperature range. This technique is used to get information about the thermal stability of the precursor and produced materials.

3. Results and Discussion

3.1 X-Ray Diffraction

Figure 1 compares the x-ray diffraction patterns from pure $\text{Al}_2(\text{MoO}_4)_3$ and the materials produced by the reaction with different quantities of cobalt in molar ratio $\text{Co}/\text{Al}_2(\text{MoO}_4)_3 = 0, 0.1, 0.2, 0.3, 0.4, 0.5, 0.6, 0.8$ and 1. The results suggest that Co, when mixed, in the solid state, with $\text{Al}_2(\text{MoO}_4)_3$ does not remain inert, but no free cobalt has been detected in any of these samples.

The x-ray diffraction patterns in Fig. 2, where 2θ is between 25° and 30°, show that a new phase Co MoO_4 ^[13,14] starts to show up beside the pure $\text{Al}_2(\text{MoO}_4)_3$ for all samples over the molar ratio range between 0.1 and 1.

With increasing the molar ratio the intensity of the diffraction peaks from the new phase increase while they decrease for $\text{Al}_2(\text{MoO}_4)_3$. This indicates that the reaction with cobalt occurs gradually at specific sites.

When the molar ratio exceeds 0.6 the phase MoO_2 ^[15] starts to appear in equilibrium with those already existing $\text{Al}_2(\text{MoO}_4)_3$ and CoMoO_4 . The formation of MoO_2 indicates that the molybdate species $(\text{MoO}_4)^{2-}$ become easier to reduce at this molar ratio. The aluminum liberated from the partial transformation of $\text{Al}_2(\text{MoO}_4)_3$ to CoMoO_4 and MoO_2 may intercalate via “soft chemistry” inside the crystal structures of the last compounds which also have open frameworks favorable to accommodate cations like Al^{3+} . It is also noted that no remarkable decomposition of $\text{Al}_2(\text{MoO}_4)_3$ into $\alpha\text{-Al}_2\text{O}_3$ and MoO_3 , due to the heating and/or cobalt adding, has been observed.

The molar ratio and the quantitative analysis given by XRD of all phases in equilibrium have been tabulated in Table 1.

3.2 FTIR Spectroscopy

Figure 3 represents comparative FTIR spectra of pure $\text{Al}_2(\text{MoO}_4)_3$ and its reaction products. The pattern of pure $\text{Al}_2(\text{MoO}_4)_3$ consists of bands at 835, 878 and 913 cm^{-1} . They can be assigned respectively to the symmetric stretch, asymmetric stretch, and bending vibration modes of Mo-O bonds in an isolated tetrahedral MoO_4 unit related to the tetrahedrally coordinated Mo species. The band at 1003 cm^{-1} in this spectrum could be assigned to the bridge Al-O-Mo.^[16-18]

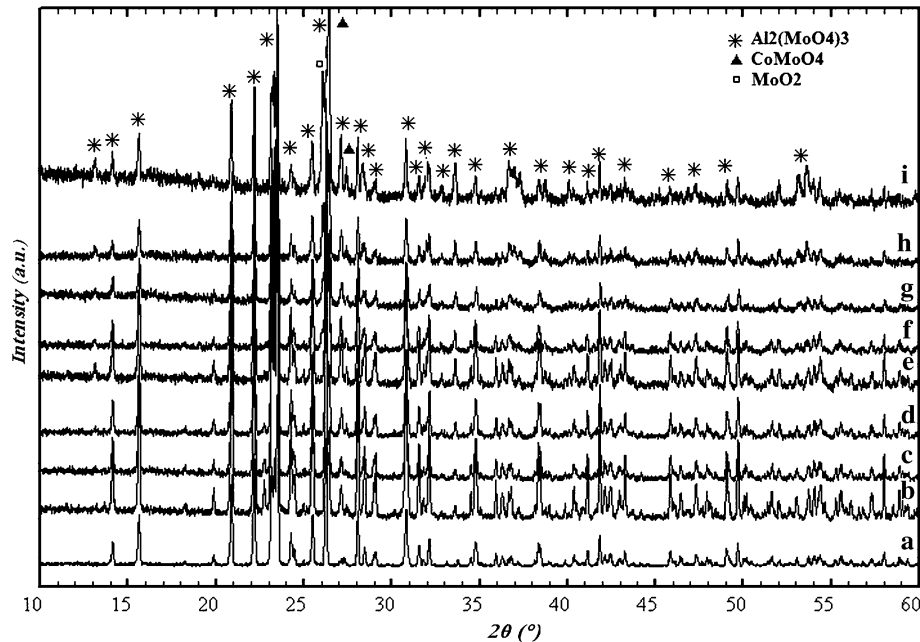


Fig. 1 X-ray diffraction patterns of pure $\text{Al}_2(\text{MoO}_4)_3$ (a), and $\text{Al}_2(\text{MoO}_4)_3$ mixed with cobalt in molar ratio: 0.1 (b); 0.2 (c); 0.3 (d); 0.4 (e); 0.5 (f); 0.6 (g); 0.8 (h); 1 (i)

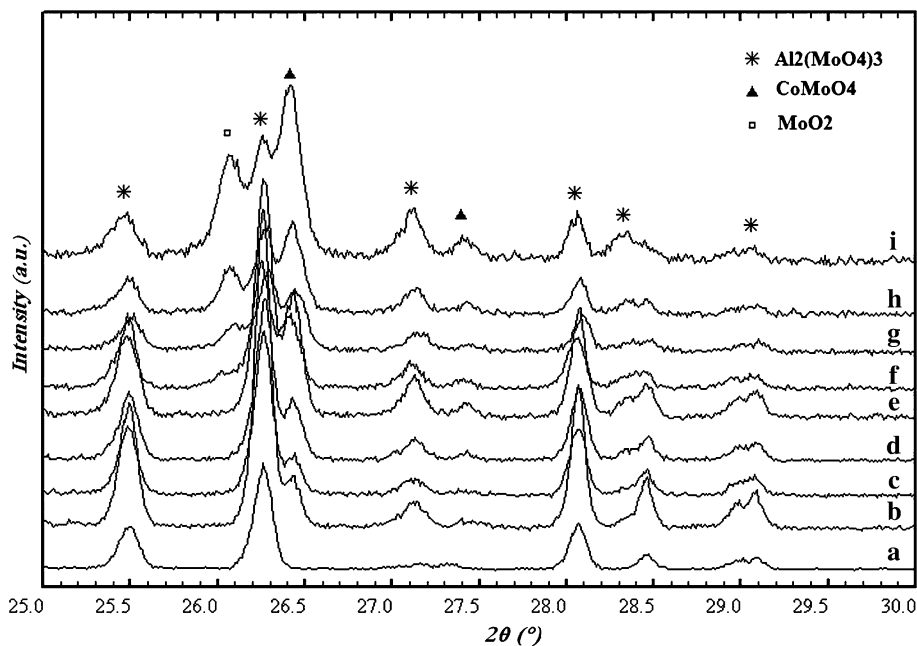


Fig. 2 X-ray diffraction patterns ($2\theta = 25\text{--}30^\circ$) of pure $\text{Al}_2(\text{MoO}_4)_3$ (a), $\text{Al}_2(\text{MoO}_4)_3$ mixed with cobalt in molar ratio: 0.1 (b); 0.2 (c); 0.3 (d); 0.4 (e); 0.6 (g); 0.8 (h); 1 (i)

Table 1 The molar ratio $\text{Co}/\text{Al}_2(\text{MoO}_4)_3$ and the quantitative analysis given by of XRD of all phases in equilibrium

Molar ratio $\text{Co}/\text{Al}_2(\text{MoO}_4)_3$	Quantitative phase analysis
0	100% $\text{Al}_2(\text{MoO}_4)_3$
0.1	98% $\text{Al}_2(\text{MoO}_4)_3$ + 2% CoMoO_4
0.2	84% $\text{Al}_2(\text{MoO}_4)_3$ + 16% CoMoO_4
0.3	82% $\text{Al}_2(\text{MoO}_4)_3$ + 18% CoMoO_4
0.4	74% $\text{Al}_2(\text{MoO}_4)_3$ + 26% CoMoO_4
0.5	70% $\text{Al}_2(\text{MoO}_4)_3$ + 30% CoMoO_4
0.6	62% $\text{Al}_2(\text{MoO}_4)_3$ + 38% CoMoO_4
0.8	60% $\text{Al}_2(\text{MoO}_4)_3$ + 39% CoMoO_4 + 1% MoO_2
1	41% $\text{Al}_2(\text{MoO}_4)_3$ + 56% CoMoO_4 + 3% MoO_2

By increasing the molar ratio the bands at 913 cm^{-1} assigned to MoO_4 become sharper indicating the increase in the concentration of this unit due to the formation of CoMoO_4 . Also one can see the appearance of small shoulders at 665 and 780 cm^{-1} which could be assigned to the formation of Co-O-Mo bond related to CoMoO_4 .^[19,20] When the molar ratio exceeds 0.6 the shoulder at 950 cm^{-1} becomes more pronounced indicating the formation of Mo=O related to MoO_2 as mentioned in the above XRD patterns. It could also be seen in this figure that the $\text{Al}_2(\text{MoO}_4)_3$ characteristic bands are always present in all the FTIR spectra without any significant shift.

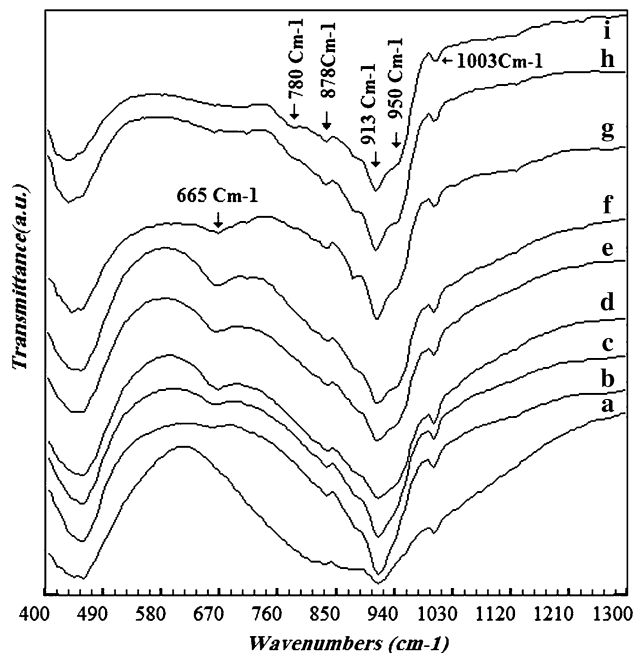


Fig. 3 FTIR spectra of pure $\text{Al}_2(\text{MoO}_4)_3$ (a), $\text{Al}_2(\text{MoO}_4)_3$ mixed with cobalt in molar ratio: 0.1 (b); 0.2 (c); 0.3 (d); 0.4 (e); 0.5 (f); 0.6 (g); 0.8 (h); 1 (i)

3.3 Thermal Behavior

The DTA curve of the precursor $\text{Al}_2(\text{MoO}_4)_3$, having a melting point at about 940°C , is presented in Fig. 4(a) but does not show any peak within the present range of

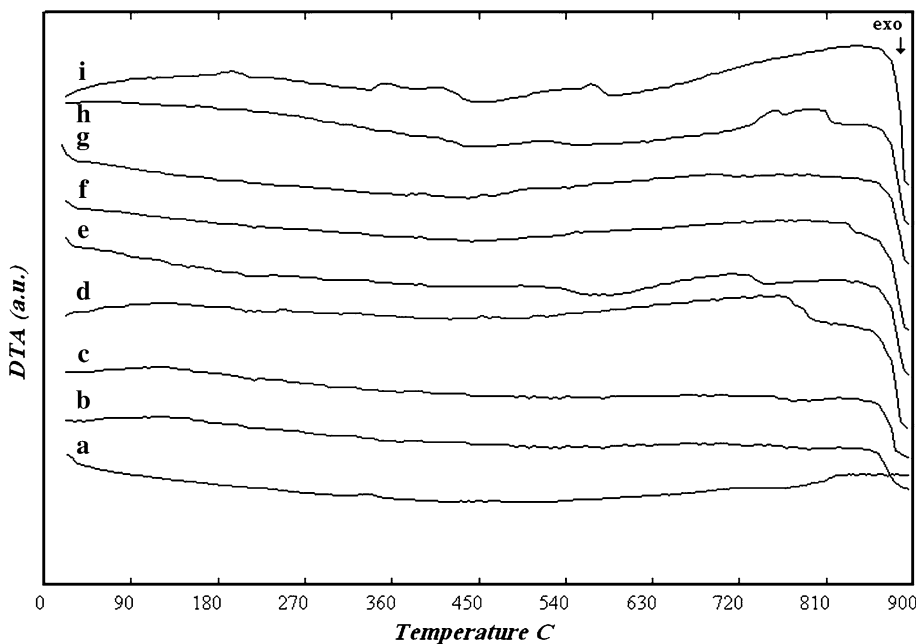


Fig. 4 DTA curves of pure $\text{Al}_2(\text{MoO}_4)_3$ (a), $\text{Al}_2(\text{MoO}_4)_3$ mixed with cobalt in molar ratio: 0.1 (b); 0.2 (c); 0.3 (d); 0.4 (e); 0.5 (f); 0.6 (g); 0.8 (h); 1 (i)

measurement between 20 and 900 °C (the maximum range of the measuring instrument). This means that $\text{Al}_2(\text{MoO}_4)_3$ is thermally stable throughout the temperature range of measurement.

The curves 4b to 4i show the appearance of peak onset at temperatures about 900 °C, lower than the melting point of pure aluminum molybdate, which could be attributed to the phase transition of the formed phase CoMoO_4 .^[21]

For samples containing molar ratio higher than 0.6, one can see some indication of other small peaks, besides that concerning the transition of CoMoO_4 in the temperature range 200-600 °C which could be related to the phase transition of the third phase MoO_2 .^[22]

The results obtained by this technique are in agreement of those obtained by x-ray diffraction and FTIR.

3.4 Isotherms and Pore Size Distribution

The nitrogen adsorption/desorption isotherms of pure $\text{Al}_2(\text{MoO}_4)_3$ and its sub products are presented in Fig. 5. The isotherm of the pure material is of type I (IUPAC classification)^[23] typical of microporous systems. A small hysteresis is clearly observed for samples containing molar ratio between 0.1 and 0.6, suggesting that the pores are mainly smooth and cylindrical, with a low contribution of mesopores. When the molar ratio exceeds the value 0.6, the isotherm becomes of type IV (characteristic of mesopores) with a small contribution of micropores which could be due to the participation of MoO_2 pores in the isotherms behavior.

The adsorption pore size distributions (PSD) calculated, on the basis of BJH method are shown in Fig. 6. This figure shows that pure $\text{Al}_2(\text{MoO}_4)_3$, with narrow pore size

distribution, had average pore diameter about 1.75-2.75 nm. For the samples where other phases have appeared, a differentiation in the pore size is noticed due to the non-uniform pore sizes relating to the co-existing phases.

As shown in Fig. 6(b)-(g), for samples consisting of molar ratio between 0.1 and 0.6, the pores are distributed in two ranges: 1.75-2.75 and 4-120 nm. For samples treated with more than 60% of cobalt the pores are distributed in three ranges: (1.75-2.75), (4-21) and (21-111) nm (Fig. 6h, i).

4. Conclusion

The reactivity, in solid state, of cobalt towards inorganic materials containing molybdate of trivalent metals such as $\text{Al}_2(\text{MoO}_4)_3$ has been investigated using x-ray diffraction, FTIR, DTA and nitrogen adsorption techniques.

Depending on the molar ratio of the $\text{Co}/\text{Al}_2(\text{MoO}_4)_3$, the results obtained revealed that the cobalt ions could be chemisorbed by aluminum molybdate where the reaction gives rise to other solid phases: CoMoO_4 and MoO_2 . The abundance of each compound depends mainly, on the molar ratio present in each specimen. From XRD analysis the peaks for CoMoO_4 and MoO_2 compounds appear gradually, their intensities increase with increasing the molar ratio.

FTIR results also confirmed the existence of these last phases beside $\text{Al}_2(\text{MoO}_4)_3$ by showing the appearance of bands characteristics to these phases.

The DTA results also give information about the thermal stability or phase transition of the phases formed

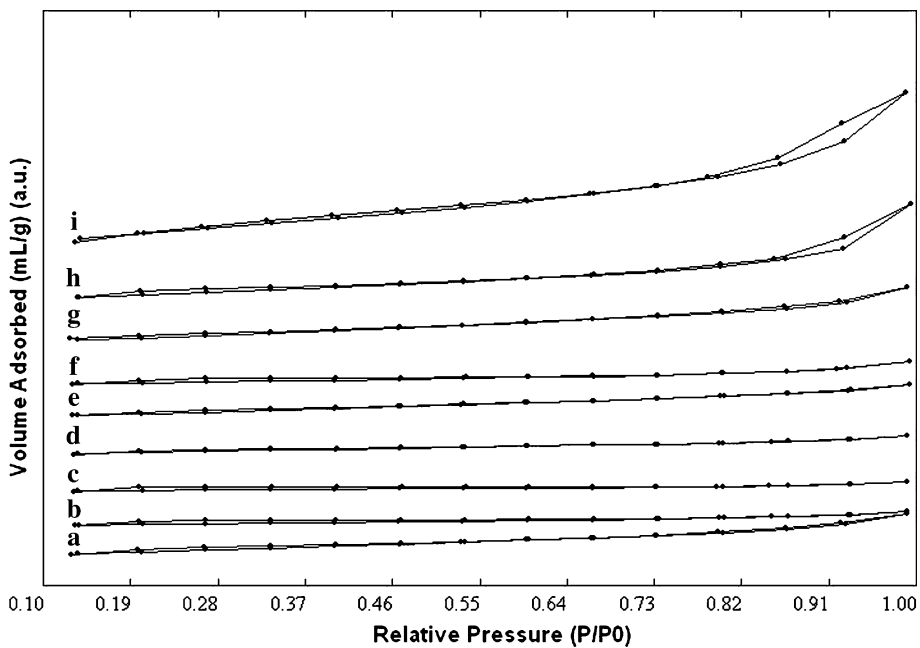


Fig. 5 Nitrogen adsorption-desorption isotherms of pure $\text{Al}_2(\text{MoO}_4)_3$ (a), $\text{Al}_2(\text{MoO}_4)_3$ mixed with cobalt in molar ratio: 0.1 (b); 0.2 (c); 0.3 (d); 0.4 (e); 0.6 (g); 0.8 (h); 1 (i)

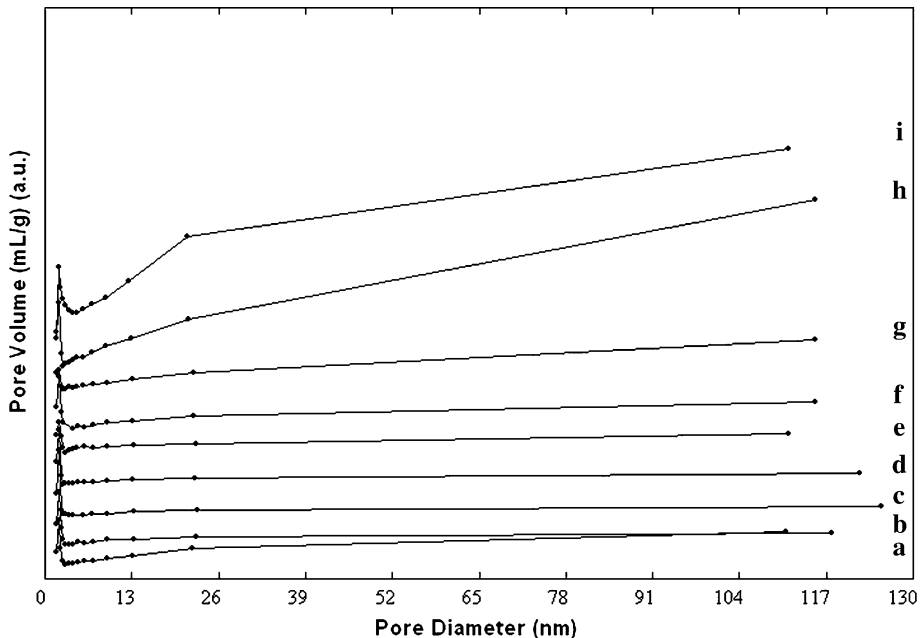


Fig. 6 Pore size distribution of pure $\text{Al}_2(\text{MoO}_4)_3$ (a), $\text{Al}_2(\text{MoO}_4)_3$ mixed with cobalt in molar ratio: 0.1 (b); 0.2 (c); 0.3 (d); 0.4 (e); 0.5 (f); 0.6 (g); 0.8 (h); 1 (i)

during the reaction of $\text{Al}_2(\text{MoO}_4)_3$ with cobalt in different molar ratio.

The adsorption-desorption isotherms described the pore uniformity in relation to the molar ratio where the total pore volume and the pore type has been modified progressively with the increasing molar ratio.

Acknowledgments

The author would like to thank Professor I. Othman, General Director of the Atomic Energy Commission of Syria as well as Dr. T. Yassin, Head of Chemistry Department for their support. Thanks are also to Dr. S. Alkhawaja

Section I: Basic and Applied Research

for the valuable discussion, Ms. H. Alsawaf and Mr. H. Harmalani for the technical helps. 0.00.0045/0.2.

References

1. P.H. Tewari and W. Lee, Adsorption of Co(II) at the Oxide-Water Interface, *J. Colloid Interf. Sci.*, 1975, **52**(1), p 77-88
2. K.R. Kim, S.H. Lee, S.W. Paek, H. Chung, and J.H. Yoo, Adsorption of Cobalt(II) Ion by Titanium-Based Oxides in High Temperature Water, *Korean J. Chem. Eng.*, 1999, **16**(1), p 34-39
3. Y.H. Kim, Adsorption of Cobalt on ZrO_2 and Al_2O_3 Absorbents in High-Temperature Water, *Sep. Sci. Technol.*, 2000, **35**(14), p 2327-2341
4. Z. Zuo, W. Huang, P. Han, and Z. Li, Theoretical and Experimental Investigation of Influence of Co and Pd on the Titanium Dioxide Phase Transition by Different Calcined Temperature, *J. Mol. Struct.*, 2009, **9**(36), p 118-124
5. H. Xiong, Y. Zhang, K.Y. Liew, and J. Li, Catalytic Performance of Zirconium Modified Co/Al_2O_3 for Fischer-Tropsch Synthesis, *J. Mol. Catal. A: Chem.*, 2005, **2**(31), p 145-151
6. P.M. Alvarez, F.J. Beltran, J.P. Pocostales, and F.J. Masa, Preparation and Structural Characterization of Co/Al_2O_3 Catalysts for the Ozonation of Pyruvic acid, *Appl. Catal. B: Environ.*, 2007, **72**, p 322-330
7. M. Fleisschhammer, M. Panthofer, and W. Tremel, The Solubility of Co in TiO_2 Anatase and Rutile and the Effect on Magnetic Properties, *Solid State Chem.*, 2009, **182**, p 942-947
8. W.T.A. Harrison, A.K. Cheetham, and J. Faber, Jr., The Crystal Structure of Aluminum Molybdate, $Al_2(MoO_4)_3$, Determined by Time-of-Flight Powder Neutron Diffraction, *J. Solid State Chem.*, 1988, **76**, p 328-333
9. M. Kassem, Phase Relations in the Al_2O_3 - MoO_3 and Al-MoO₃ Systems, Investigated by X-Ray Powder Diffraction, FTIR and DTA Techniques, *Inorg. Mater.*, 2006, **42**(2), p 1-6
10. Stoe WinXpow 32, Stoe and Cie GmbH, Darmstadt, Germany, 2008
11. K. Sing, The Use of Nitrogen Adsorption for the Characterization of Porous Aterials, *Colloid Surf. A: Physicochem. Eng. Asp.*, 2001, **187-188**, p 3-9
12. J.C. Groen, L.A.A. Peffer, and J. Perez-Ramirez, Pore size Determination in Modified Micro- and Mesoporous Materials-Pitfalls and Limitation in Gas Adsorption Data Analysis, *Microporous Mesoporous Mater.*, 2003, **60**, p 1-17
13. M. Hu, Y. Murakami, M. Ogura, S. Maruyama, and T. Okubo, Morphology and Chemical State of Co-Mo Catalysts for Growth of Single-Walled Carbon Nanotubes Vertically Aligned on Quartz Substrates, *J. Catal.*, 2004, **225**, p 230-239
14. A.A. Zahran, W.M. Shaheen, and G.A.E. Shobaky, Surface and Catalytic Properties of MoO_3/Al_2O_3 System Doped with Co_3O_4 , *Mater. Res. Bull.*, 2005, **40**, p 1065-1080
15. B.G. Brandt and A.C. Skapski, A Refinement of Crystal Structure of Molybdenum Dioxide, *Acta Chem. Scand.*, 1967, **21**, p 661
16. S. Xie, K. Chen, A.T. Bell, and E. Iglesia, Structural Characterization of Molybdenum Oxide Supported on Zirconia, *J. Phys. Chem. B*, 2000, **104**, p 10059-10068
17. F. Lei, B. Yam, and H.H. Chen, Solid-State Synthesis, Characterization and Luminescent Properties of Eu^{3+} -Doped Gadolinium Tungstate and Molybdate Phosphors: $Gd_{(2-x)}MO_6: Eu_x^{3+}$ ($M = W, Mo$), *J. Solid State Chem.*, 2008, **181**, p 2845-2851
18. J.B. Sohn, E.W. Chun, and Y. Il Pae, Spectroscopic Studies on ZrO_2 Modified with MoO_3 and Activity for Acid Catalysis, *Bull. Korean Chem. Soc.*, 2003, **24**(12), p 1785
19. N. Gabriel Armatas, D.G. Allis, A. Prosvirin, G. Carnutti, C.J. O'Connor, K. Dunbar, and J. Zubietta, Molybdophosphonate Clusters as Building Blocks in the Oxomolybdate-Organodiphosphonate/Cobalt(II)-Organoimine System: Structural Influences of Secondary Metal Coordination references and Diphosphonate Tether Lengths, *Inorg. Chem.*, 2008, **47**, p 832-854
20. F.J. Gil Llabias, A. Lopez Agudo, and V. Rives-Arnau, Characterization of Oxide $Co-Mo/\gamma-Al_2O_3$ Hydrodesulphurization Catalysts Prepared by Different Method, *J. Mater. Sci.*, 1982, **17**(4), p 936-946
21. S. Kin'ya, O. Kiyoshi, O. Massaki, and K. Yoshihide, Formation and Phase Transition of Cobalt Molybdate in Cobalt Oxide-Molybdenum Trioxide-Alumina System, *J. Solid State Chem.*, 1979, **27**(2), p 215-225
22. K.T. Jacob, V.S. Saji, J. Gopalakrishnan, and Y. Waseda, Thermodynamic Evidence for Phase Transition in $MoO_2-\delta$, *J. Chem. Thermodyn.*, 2007, **39**, p 1539-1545
23. K.S.W. Sing, D.H. Everett, R.A.W. Haul, L. Moscou, R.A. Pierotti, J. Rouquerol, and T. Sieminska, Reporting Physisorption Data For Gas/Solid Systems with Special Reference to the Determination of Surface Area and Porosity, *Pure Appl. Chem.*, 1985, **57**, p 603-619